

Static, dynamic and fatigue behavior of newly designed stem shapes for hip prosthesis using finite element analysis

A. Zafer Senalp *, Oguz Kayabasi, Hasan Kurtaran

Gebze Institute of Technology, Department of Design and Manufacturing Engineering, PK. 141, 41400 Gebze/Kocaeli, Turkey

Received 20 September 2005; accepted 14 February 2006

Available online 19 April 2006

Abstract

Forces applied to the implant due to human activity generate dynamic stresses varying in time and resulting in the fatigue failure of implant material. Therefore, it is important to ensure the hip prostheses against static, dynamic and fatigue failure. Finite element method has been used in orthopedic biomechanics as an important tool in the design and analysis of total joint replacements and other orthopedic devices. In this study, four stem shapes of varying curvatures for hip prosthesis were modeled. Static, dynamic and fatigue behavior of these designed stem shapes were analyzed using commercial finite element analysis code ANSYS. Static analyses were conducted under body load. Dynamic analyses were performed under walking load. Pro/Engineer was used for CAD modeling of the stem shapes. Fatigue behavior of stem shapes was predicted using ANSYS Workbench software. Performance of the stem shapes was investigated for Ti–6Al–4V and cobalt–chromium metal materials and compared with that of a commonly used stem shape developed by Charnley. Published by Elsevier Ltd.

Keywords: Femur; Implant; Stem; Fatigue; Dynamic analysis; Finite element method

1. Introduction

Total hip replacement is successfully applied to the patients affected by hip diseases [1–4]. Forces applied to the prosthesis due to human activity generate dynamic stresses varying in time and resulting in the mechanical fatigue failure of implant material. Therefore it is important to ensure the hip prostheses against fatigue failure. The fatigue failure of hip prostheses was reduced significantly in the past two decades [5,6]. However, every new implant design has to be ensured against the fatigue failure. Performance and success of long-term survival of cemented total hip arthroplasty (THA) is related to the attachment of the prosthesis to the bone. Cement–metal interface failures, separation of the stem–cement interface and fractures in the cement may initiate the initial loss of the fixation of the implant [7]. Particularly, interface debonding and cement fatigue failure are now likely to cause long-term loosening

of the implant, according to damage accumulation failure scenario for cemented THA stems [8]. If the stem shape design leads to high stresses in fixation areas of the prosthesis, fracture in short term or fatigue failure in long term of the prosthesis is quite likely to occur. Several researches have been conducted to investigate the stress and fatigue behavior of prostheses under static body load conditions.

In the literature, to simulate fatigue damage of implant, finite element models in association with cement damage algorithms have been used [9,10]. In several previous works [9,11–15], three-dimensional analysis of the mechanical interaction between a femoral stem and the femur in a hip arthroplasty was performed. The standard femur geometry was used to produce the finite element mesh of the cortical and cancellous bone. Similarly in another study [16] a quasi three-dimensional finite element model for fatigue analysis of the hip implant was initially developed. The side-plate concept was introduced to account for the three-dimensional structural integrity of the cement and cortical bone and to recover the hoop stress in the cement mantle as membrane stress. This was achieved by an appropriate calibra-

* Corresponding author. Tel.: +90 262 653 84 97; fax: +90 262 653 06 75.
E-mail address: zsenalp@gyte.edu.tr (A.Z. Senalp).

tion of the geometric parameters. Two different damage rules; linear and non-linear, were proposed to produce two different damage evolution algorithms for the estimation of the fatigue lifetime. In another work by the same author, the generated algorithm was implemented in the finite element code ABAQUS [17].

In this work, the fatigue analyses of four different implant geometries were performed. For the analysis three-dimensional model of femur, cement and implant were constructed. The implant and bone-cement were designed according to femur geometry. By using these geometric models finite element models were constructed. The analyses were performed using ANSYS Workbench finite element software. Two different material properties were tested for each geometry type. In order to determine the behavior of the implant walking load was used. In the analysis, a viscoelastic material model is utilized for bone-cement. At the end of the analyses, the most appropriate geometry type and material for the implant that should withstand to fatigue loading was determined.

2. CAD and finite element model

2.1. CAD model

Stem shapes have significant influence on the performance of prostheses. Stem shapes with smooth surfaces generally reduce stress concentrations and lead to high fatigue life of the prosthesis. Stem shapes with sharp or non-smooth surfaces provide good bonding capability at the interface and prevent possible sliding at the interface. The level of stress concentration and tendency for fatigue failure depend on the sharpness of the stem surfaces. In this study, four different stem shapes with varying surface curvatures are designed to achieve both good bonding capability at the interface and high fatigue life of the prosthesis. The stem shapes those were analyzed in this study are shown in Fig. 1.

For the femur geometry the standardized model of Viceconti et al. [18] was used. The IGES data of femur was imported into Pro/Engineer and solid model of the femur was created after truncating the model. CAD model of the complete prosthesis is imported into ANSYS 8.0 pre-processing environment to create the finite element model required in the analyses. Stem shapes have diameters of 15 mm and 10 mm at thick and thin sections, respectively. Stem lengths are 85 mm. The bone-cement mantle is approximately 4 mm. Curved stem has radius of 50 mm. Notched stem has corner radius of 3 mm.

2.2. Finite element model

Finite element model required in FE analysis is created by discretizing the geometric models shown in Fig. 1 into smaller and simpler elements. The discretization was performed in ANSYS environment. The three-dimensional solid model assembly of femur, bone-cement and implant was transferred to ANSYS Workbench by direct interface. ANSYS Workbench automatically recognizes the contacts existing between each part and establishes the contact conditions for corresponding contact surfaces.

To build the finite element model, femur, bone-cement and implant were meshed using a higher order three-dimensional solid element; SOLID187 which has a quadratic displacement behavior and is well suited to modeling irregular meshes (such as those produced from various CAD/CAM systems). The element is defined by 10 nodes having three degrees of freedom at each node: translations in the nodal x , y , and z directions [19].

For modeling the contact and sliding between femur–bone-cement interface and the bone-cement–implant interface, CONTA174 and TARGE170 elements were used. CONTA174 element was located on the surfaces of 3-D solid element, SOLID187. TARGE170 is used to represent various 3-D “target” surfaces for the associated contact

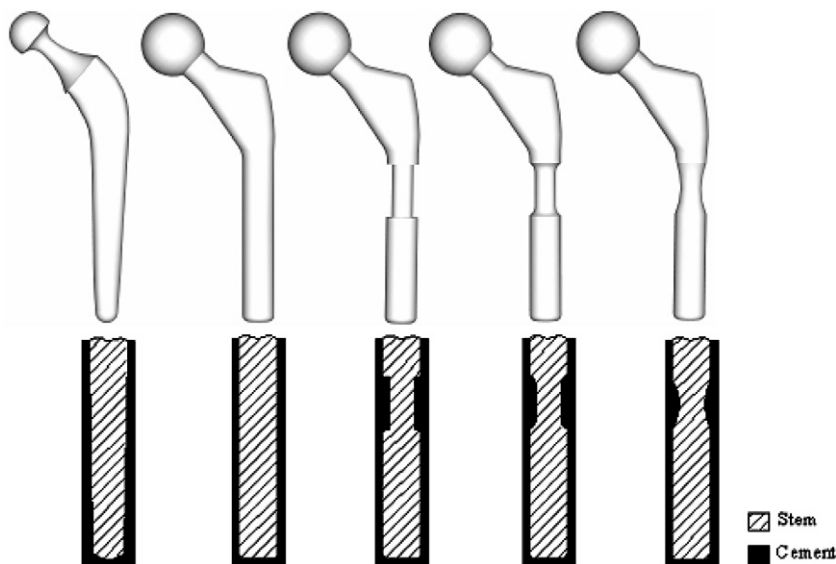


Fig. 1. Stem types (Charnley, straight, notched and curved).

element CONTA174. The contact elements themselves overlay the solid elements describing the boundary of a deformable body and are potentially in contact with the target surface, defined by TARGE170. CONTA174 has the same geometric characteristics as the solid element face with which it is connected. Contact occurs when the element surface penetrates one of the target segment elements (TARGE170) on a specified target surface. Coulomb and shear stress friction are allowed.

Completely bonded contact type was chosen as contact condition for contact surfaces. According to Nuno and Avanzoli [20], the coefficient of friction was experimentally measured between 0.17 and 0.32 for polished or satin finish stem surface and bone-cement material poly methyl methacrylate (PMMA). The coefficient of friction value of 0.2 was used in this study.

Three different finite element models, each consisting different implant type were prepared. Each complete model consisted of around 72,458 elements and 88,000 nodes. The femur consisted of 7800 elements, the bone-cement consisted of 8700 elements and the implant consisted of 40,000 elements. The rest of about 16,000 elements were used for contact and target elements. Fine mesh was applied to the implant models. The finite element model of the femur, the bone-cement and the implant are shown in Fig. 2.

2.3. Material models

Two different materials for implant were used in the finite element simulation. These materials are Ti-6Al-4V and cobalt-chromium alloy. Behaviors of these materials are represented with linear isotropic material models. Mechanical properties of Ti-6Al-4V and cobalt-chromium alloy are shown in Table 1. The alternating stress versus number of cycles (*S-N* curve) for implant materials used in this study for fatigue calculations was given in logarithmic scale in Fig. 3.

To account for the effect of the bone behavior on the prosthesis accurately, inner and outer sides of the bone (cancellous bone and cortical bone) are modeled with different material properties. Inner side of the bone (cancellous bone) is represented with transversely isotropic

Table 1
Mechanical properties of stem materials

Material	Young's modulus (GPa)	Poisson ratio (ν)	Yield strength (MPa)
Ti-6Al-4V	110	0.32	800
Cobalt-chromium alloy	220	0.30	720

material model ($E_x = E_y = 11.5$ GPa, $E_z = 17$ GPa; $G_{xy} = 3.6$ GPa, $G_{xz} = G_{yz} = 3.3$ GPa; $\nu_{xy} = 0.51$, $\nu_{xz} = \nu_{yz} = 0.31$ GPa) [21]. Outer side of the bone (cancellous bone) is modeled with linear isotropic material model of $E = 2.13$ GPa and $\nu = 0.3$. Cement (polymethyl methacrylate) is modeled with linear isotropic material model of $E = 2.7$ GPa and $\nu = 0.35$ [20]

$$\dot{\epsilon}_{cr} = 5.168 \times 10^{-6} \sigma^{1.858} t^{-0.717} \quad [21,22], \quad (2.1)$$

where $\dot{\epsilon}_{cr}$ is the creep strain rate, σ the equivalent Von Mises stress (MPa), and t the time at end of substep (h).

2.4. Loading conditions

For static analysis, a load of 3 kN (F_{static}) with an angle of 20° is applied on the surface of the implant bearing as shown in Fig. 3. Static load represents a person of 70 kg [23]. An abductor muscle load of 1.25 kN ($F_{abductor\ muscle}$) is applied at an angle of 20° to the proximal area of the

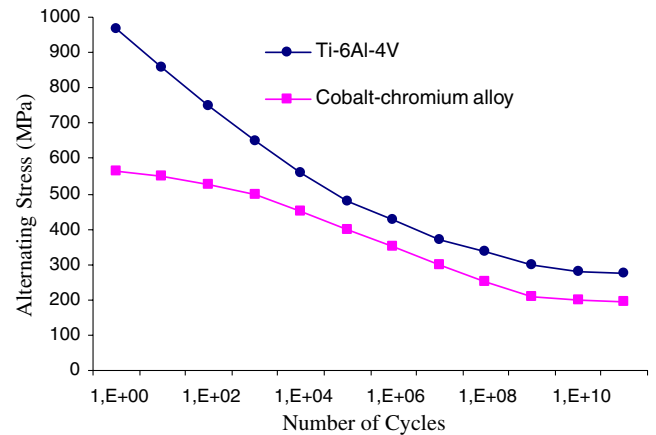


Fig. 3. *S-N* curve for implant materials; Ti-6Al-4V and cobalt-chromium alloy.

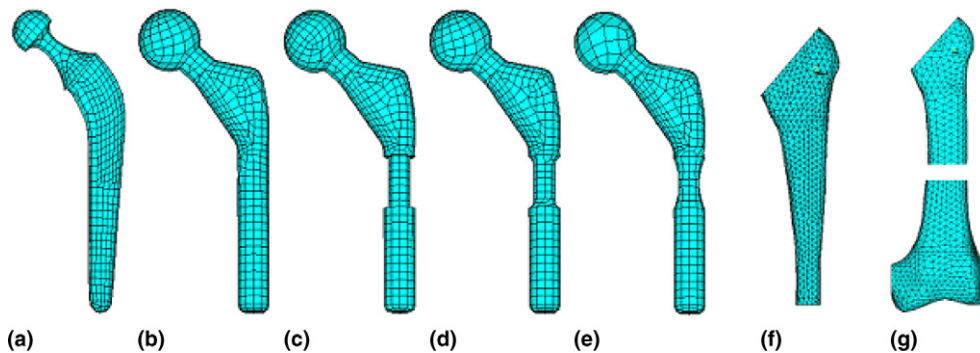


Fig. 2. Finite element models of (a) Charnley stem shape, (b) Stem-1, (c) Stem-2, (d) Stem-3, (e) Stem-4, (f) bone-cement and (g) femur.

greater trochanter. An ilio tibial-tract load of 250 N ($F_{\text{ilio tibial-tract}}$) is applied to the bottom of the femur in the longitudinal femur direction. Distal end of the femur is constrained not to move in horizontal direction.

For dynamic analysis, time-dependent walking load (F_{dynamic}) is applied as shown in Fig. 4. Time history of the dynamic load components for 5 s is demonstrated in Fig. 5.

3. Finite element analysis and results

Static and dynamic analyses of the prosthesis should be conducted to ensure about the safety of the design. In the literature, prostheses are often designed according to the results of static analysis. Static finite element (FE) analyses are mostly conducted under body weight loads. However, dynamic effects may add up to about 10–20% or more loading to the prosthesis which must be taken into account not

to cause fracture or fatigue failure of the prosthesis. To investigate how static and dynamic analysis results differ from each other, prosthesis is analyzed under static body weight load and dynamic walking load.

Finite element analyses of the prosthesis are carried out using ANSYS on a P4 2.0 GHz Intel processor PC. Analyses take about 20 h of CPU time. Von Mises stresses in the stem shapes resulted from static and dynamic finite element analyses are shown in Figs. 6–9.

It is important that the maximum equivalent stress on the prostheses should be lower than the endurance limit of the prosthesis materials for safety. The calculated Von Mises stresses as shown in Table 2 are much lower than the yield stresses of Ti-6Al-4V and cobalt–chromium alloy given in Table 1. This means, prosthesis with all stems is safe for stress condition.

4. Fatigue analysis

A good implant design should satisfy maximum or an infinite fatigue life. This can only be ensured by physical testing or a fatigue analysis. In this study, fatigue life of the prosthesis upon finite element stress analysis is predicted using the computer code of ANSYS Workbench [19]. Fatigue calculations of the implant are conducted for Ti-6Al-4V and cobalt–chromium alloy materials. In fatigue calculations, fatigue material models shown in Fig. 9 are used. Fig. 9 known as *S-N* curves shows fatigue properties of Ti-6Al-4V and cobalt–chromium alloy in

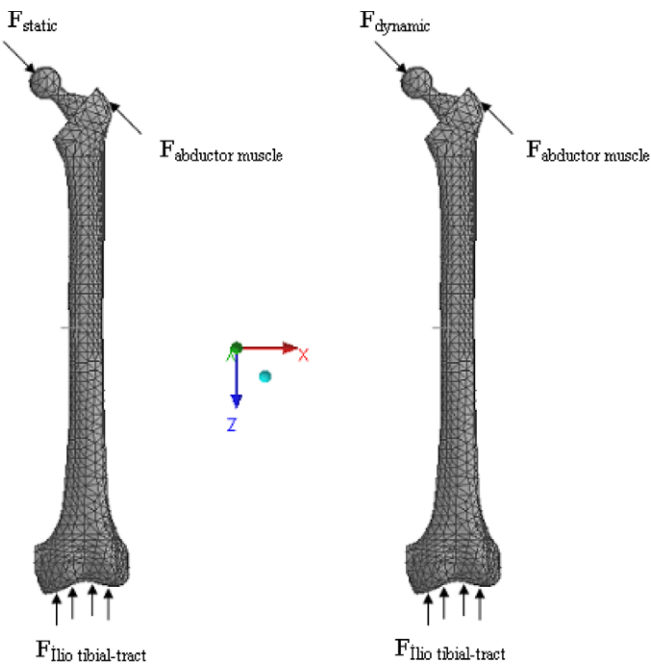


Fig. 4. Applied forces on the bone-cement-prosthesis assembly.

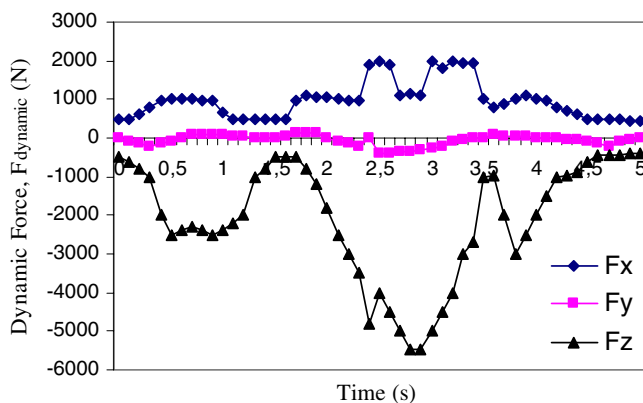


Fig. 5. Time history of walking load components on the prosthesis.

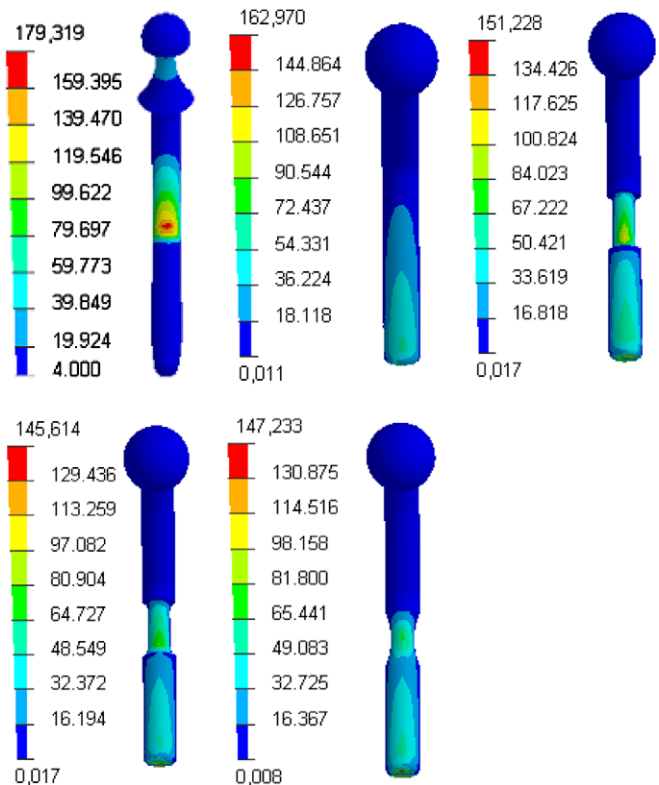


Fig. 6. Stress distribution on the stem shapes under static loading for Ti-6Al-4V material.

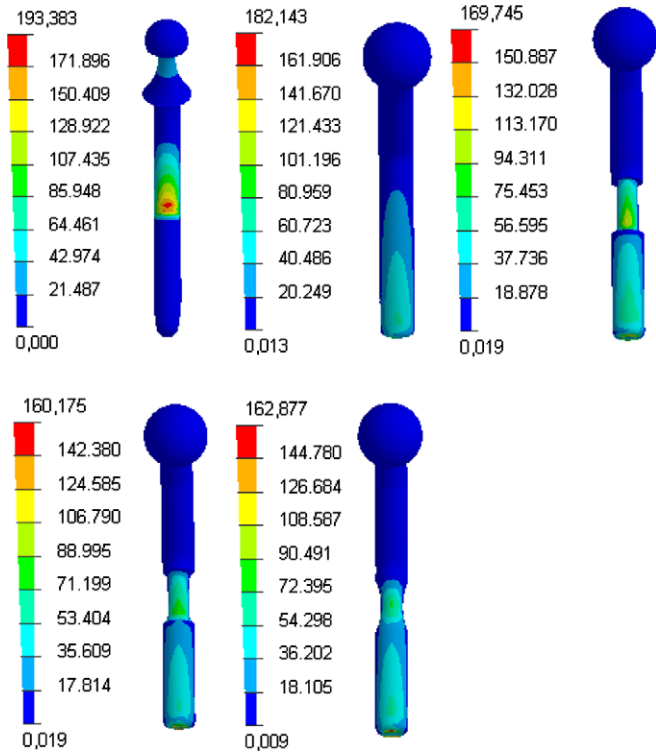


Fig. 7. Stress distribution on the stem shapes under static loading for cobalt-chromium material.

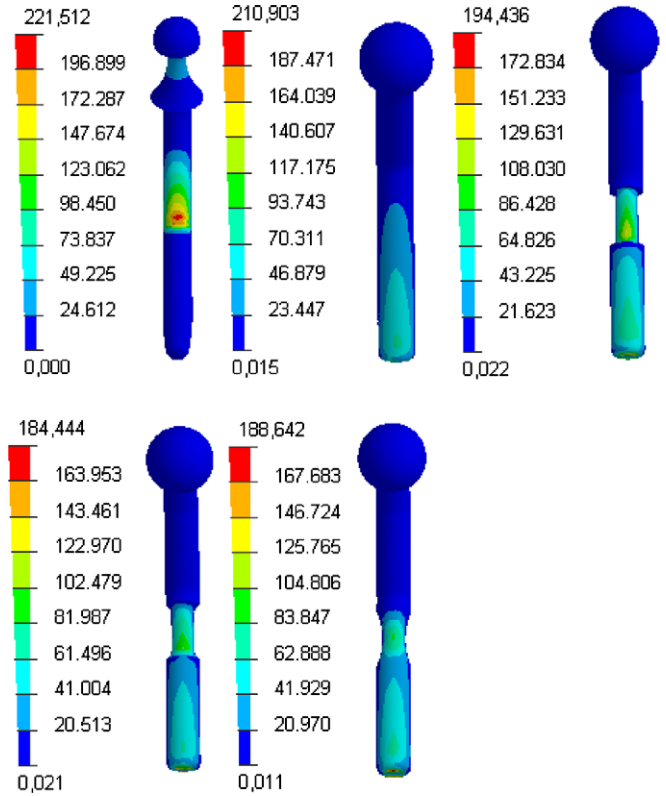


Fig. 9. Maximum stresses that occur on the stem shapes under dynamic loading for cobalt-chromium material (time = 2.7 s).

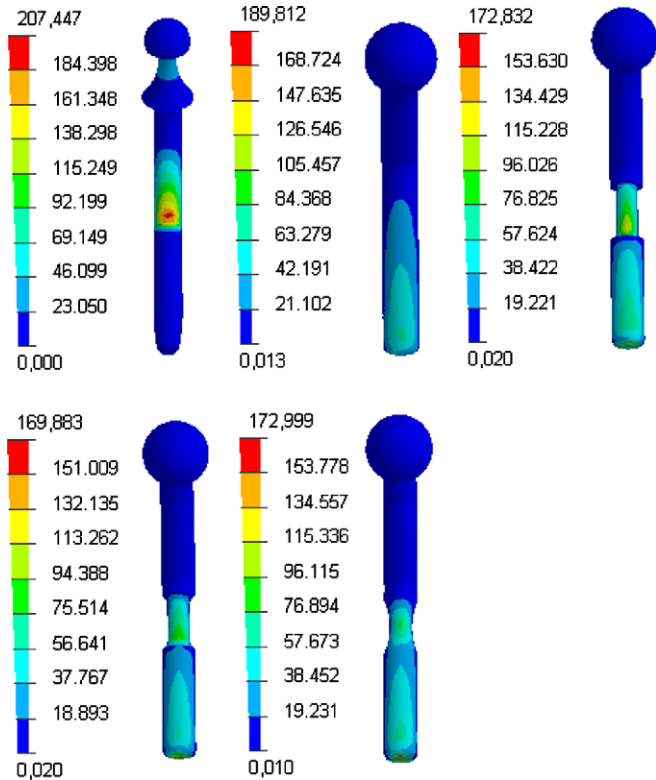


Fig. 8. Maximum stresses that occur on the stem shapes under dynamic loading for Ti-6Al-4V material (time = 2.7 s).

Table 2

Maximum Von Mises stresses of stem shapes under static and dynamic loading

Stem shapes	Maximum Von Mises stress (static) (MPa)		Maximum Von Mises stress (dynamic) (MPa)	
	Ti-6Al-4V	Cobalt-chromium	Ti-6Al-4V	Cobalt-chromium
Charnley	179.3	193.4	207.4	221.5
Stem-1	162.9	182.1	189.8	210.9
Stem-2	151.2	169.7	172.8	194.4
Stem-3	145.6	160.2	169.9	184.4
Stem-4	147.2	162.9	172.9	188.6

terms alternating stress versus number of cycles. Fatigue life of prosthesis is calculated based on Goodman, Soderberg, Gerber and mean-stress fatigue theories.

Stress life (S/N) approach was used for determining the fatigue life of the implant materials. This approach is useful for the initial process of materials selection of implant materials that will be subjected to high cyclic loading conditions. The advantage of this approach is that it represents both initiation and propagation of cracks in the aggressive environment [24].

In the finite element model, the materials (bone, metal and cement) are considered to be elastic and the analysis was performed according to infinite life criteria (10^9 cycles). Therefore, the stress amplitude was ensured to be lower than the lowest stress on the SN curve.

Fatigue analyses were performed according to Goodman, Soderberg, Gerber and mean-stress curve options. Mean stress σ_m is defined as

$$\sigma_m = \frac{(\sigma_{\max} + \sigma_{\min})}{2} \quad (4.1)$$

and alternating stress as

$$\sigma_a = \frac{(\sigma_{\max} - \sigma_{\min})}{2} \quad (4.2)$$

According to Goodman theory any combination of mean and alternating stress that lies on or below the Goodman line which is defined by

$$\left(\frac{\sigma_a}{S_e}\right) + \left(\frac{\sigma_m}{S_u}\right) = \frac{1}{N} \quad (4.3)$$

will have infinite life. Here N stands for safety factor, S_e for endurance limit and S_u for ultimate tensile strength of the material. According to Soderberg approach any combination of mean and alternating stress that lies on or below the Solderberg line defined by

$$\left(\frac{\sigma_a}{S_e}\right) + \left(\frac{\sigma_m}{S_y}\right) = \frac{1}{N} \quad (4.4)$$

will have infinite life. Where S_y is the yield strength of material. Unlike Goodman and Soderberg, Gerber approach is not linear in form and Gerber line is defined by the equation

$$\left(\frac{N\sigma_a}{S_e}\right) + \left(\frac{N\sigma_m}{S_u}\right)^2 = 1 \quad (4.5)$$

under which is defined to be safe region. The Goodman, Soderberg and Gerber options use static material properties along with S – N data to account for any mean stress while mean-stress curve option offered by ANSYS uses experimental fatigue data to account for mean stress.

During the simulation process, all input data was prepared using finite element Von Mises stresses in the femur, bone-cement, implant and bone-cement–implant interface were calculated.

5. Fatigue analysis results

Von Mises stresses obtained from finite element analyses are utilized in fatigue life calculations. All fatigue analyses are performed according to infinite life criteria (i.e., $N = 10^9$ cycles). Minimum safety factors for the prostheses based on infinite life criteria are given in Tables 3 and 4 for Ti–6Al–4V and cobalt–chromium alloy materials under static loading condition.

From Tables 3 and 4, it is seen that all new stem shapes have higher safety factor values than Charnley's stem shape according to all fatigue criteria. This means that new stem shapes are better and have higher fatigue lives than Charnley's stem shape when static loading case is considered. Among new stem shapes, Stem-3 and Stem-4 are better than the others in fatigue life. Stem-3 is the best of all. This

Table 3

Minimum safety factor of stem shapes for Ti–6Al–4V material (static analysis)

Fatigue theories	Minimum safety factor				
	Charnley	Stem-1	Stem-2	Stem-3	Stem-4
Mean stress curve	2.74	2.94	3.08	3.27	3.24
Goodman	2.23	2.41	2.54	2.67	2.65
Soderberg	2.18	2.37	2.49	2.62	2.60
Gerber	2.65	2.85	2.98	3.16	3.14

Table 4

Minimum safety factor of stem shapes for cobalt–chromium alloy material (static analysis)

Fatigue theories	Minimum safety factor				
	Charnley	Stem-1	Stem-2	Stem-3	Stem-4
Mean stress curve	1.92	2.05	2.16	2.29	2.26
Goodman	1.56	1.68	1.77	1.86	1.85
Soderberg	1.25	1.66	1.74	1.85	1.82
Gerber	1.86	2.00	2.10	2.21	2.19

Table 5

Minimum safety factor of stem shapes for Ti–6Al–4V material (dynamic analysis)

Fatigue theories	Minimum safety factor				
	Charnley	Stem-1	Stem-2	Stem-3	Stem-4
Mean stress curve	2.20	2.35	2.46	2.61	2.59
Goodman	1.78	1.92	2.03	2.13	2.10
Soderberg	1.74	1.90	1.99	2.10	2.08
Gerber	2.12	2.28	2.38	2.54	2.51

Table 6

Minimum safety factor of stem shapes for cobalt–chromium alloy material (dynamic analysis)

Fatigue theories	Minimum safety factor				
	Charnley	Stem-1	Stem-2	Stem-3	Stem-4
Mean stress curve	1.53	1.64	1.72	1.84	1.80
Goodman	1.25	1.35	1.42	1.48	1.40
Soderberg	1.00	1.32	1.40	1.48	1.45
Gerber	1.49	1.60	1.68	1.77	1.75

is true for both Ti–6Al–4V and cobalt–chromium alloy materials. The best stem shape for fatigue under static loading is Stem-3 made of Ti–6Al–4V material.

Safety factors for Ti–6Al–4V and cobalt–chromium alloy materials under dynamic loading condition are illustrated in Tables 5 and 6, respectively. Again as in static loading case, Stem-3 and Stem-4 are better than the others. Stem-3 is the best of all if it is made of Ti–6Al–4V material. Safety factor also differ under static and dynamic loading conditions. This indicates that stem shapes predicted to be safe against fatigue under static loading may fail under dynamic repetitive loadings.

6. Conclusion

The aim of this study was to determine the fatigue endurance of cemented implant. In this study, four different stem

shapes for hip prosthesis are designed. Stem shapes have geometries of varying curvatures. First stem has standard straight geometry. The other two have notched geometries and the last one has curved geometry. The notched and curved types are designed to reduce sliding of the implant in the bone-cement and to stick the implant to the bone-cement securely. Static and dynamic FE analyses of stems have been conducted using ANSYS. Based on static and dynamic FE analysis results, safety factors for fatigue life have been calculated. Fatigue calculations have been carried out for Ti–6Al–4V and cobalt–chromium alloy materials based on Goodman, Soderberg, and Gerber fatigue theories. All calculations are performed according to the infinite fatigue life criteria.

Finite element analyses in this study show that all stem shapes are safe against fatigue failure. The best stem shape for fatigue under static loading is Stem-3 made of Ti–6Al–4V material. Stem-3 made of Ti–6Al–4V material is also best under dynamic loading. However, safety factors differ under static and dynamic loading conditions. This indicates that stem shapes predicted to be safe against fatigue under static loading may fail under dynamic repetitive loadings.

References

- [1] Savilahti S, Myllyneva I, Pajamaki KJJ, Lindholm TS. Survival of Lubinus straight (IP) and curved (SP) total hip prostheses in 543 patients after 4–13 years. *Arch Orthop Trauma Surg* 1997;116:10–3.
- [2] Marston RA, Cobb AG, Bentley G. Stanmore compared with Charnley total hip replacement: a prospective study of 413 arthroplasties. *J Bone Joint Surg* 1996;78-B:178–84.
- [3] Neumann L, Freund KG, Sorenson KH. Long-term results of Charnley total hip replacement. Review of 92 patients at 15 to 20 years. *J Bone Joint Surg* 1994;76B:245–51.
- [4] Delaunay CP, Kapandji AI. Primary total hip arthroplasty with the Karl Zwemuller first-generation cementless prosthesis: a 5 to 9 year retrospective study. *J Arthroplasty* 1996;11:643–52.
- [5] Sotereanos NG, Engh CA, Glassman AH, Macalino GE. Cementless femoral components should be made from cobalt chrome. *Clin Orthop* 1995;313:146–53.
- [6] Wroblewski BM, Sidney PD. Charnley low friction arthroplasty of the hip. Long term result. *Clin Orthop* 1993;292:191–201.
- [7] Harrigan TP, Harris WH. A three-dimensional non-linear finite element study of the effect of cement–prosthesis debonding in cemented femoral total hip components. *J Biomech* 1991;24:1047–1058.
- [8] Jasty M, Malone WJ, Bragdon CR, O'Connor D, Haire T, Harris WH. The initiation of failure in cemented femoral components of hip arthroplasties. *J Bone Joint Surg* 1991;73B:551–8.
- [9] Verdonschot N, Huiskes R. The effects of cement–stem debonding in THA on the long-term failure probability of cement. *J Biomech* 1997;30:795–802.
- [10] Dolinski K. Fatigue reliability assessment of cemented hip prosthesis. *J Theor Appl Mech* 1999;3:505–18.
- [11] Andress HJ, Kahl S, et al. Clinical and finite element analysis of a modular femoral prosthesis consisting of a head and stem component in the treatment of pertrochanteric fractures. *J Orthop Trauma* 2000;14(8):546–53.
- [12] Stolk J, Verdonschot N, et al. Stair climbing is more detrimental to the cement in hip replacement than walking. *Clin Orthop* 2002;294–305.
- [13] Lennon AB, McCormack BA, et al. The relationship between cement fatigue damage and implant surface finish in proximal femoral prostheses. *Med Eng Phys* 2003;25(10):833–41.
- [14] Stolk J, Maher SA, et al. Can finite element models detect clinically inferior cemented hip implants? *Clin Orthop* 2003(409):138–150.
- [15] Waide V, Cristofolini L, et al. Modelling the fibrous tissue layer in cemented hip replacements: experimental and finite element methods. *J Biomech* 2004;37(1):13–26.
- [16] Colombi P. Fatigue analysis of cemented hip prosthesis: model definition and damage evolution algorithms. *Int J Fatigue* 2002;24:895–901.
- [17] Colombi P. Fatigue analysis of cemented hip prosthesis: damage accumulation scenario and sensitivity analysis. *Int J Fatigue* 2002;24:739–46.
- [18] Viceconti M, Casali M, Massari B. The standardized femur program. *J Biomech* 1996;29:1241.
- [19] ANSYS. ANSYS Theory Reference Manual, Release 8.0 ANSYS Inc.; 2003.
- [20] Nuno N, Avanzoli G. Residual stress at the stem-cement interface of an idealized cemented hip stem. *J Biomech* 2002;35:849–52.
- [21] Norman TL, Thyagarajan G, Saligrama VC, Gruen TA, Blaha JD. Stem surface roughness alters creep induced subsidence and 'taper-lock' in a cemented femoral hip prosthesis. *J Biomech* 2001;34:1325–33.
- [22] Chwirut JD. Long term compressive creep deformation and damage in acrylic bone cements. *J Biomed Mater Res* 1984;18:25–37.
- [23] El-Sheikh HF, MacDonalds BJ, Hashmi MSJ. Material selection in the design of the femoral component of cemented total hip replacement. *J Mater Process Technol* 2002;122:309–17.
- [24] Teoh SH. Fatigue of biomaterials: a review. *Int J Fatigue* 2000;22:825–37.